

## Direct Excitation of Nuclear Energy States in Carbon by 96-Mev Protons\*

K. STRAUCH AND F. TITUS

*Harvard University, Cambridge, Massachusetts*

(Received March, 29 1956)

The scattering of 96-Mev protons from a carbon target has been investigated at laboratory angles between  $3^\circ$  and  $90^\circ$ . At the larger scattering angles, besides the elastic peak and inelastic continuum, inelastic peaks are found whose magnitude compares with the elastic peak. These inelastic proton peaks correspond to an excitation energy of the target nucleus of 4.4, 9.6, and 20.8 Mev. The angular distribution of elastically scattered protons shows slight diffraction minima at  $40^\circ$  and  $64^\circ$  (center-of-mass) after a careful separation of elastic from inelastic protons is made. The inelastic protons are peaked in the forward direction. Possible interaction models are discussed.

### I. INTRODUCTION

THE basic concepts of the mechanism of high-energy nuclear reactions first presented by Serber<sup>1</sup> are expected to apply to the interaction of 96-Mev protons with complex nuclei. Such protons have a DeBroglie wavelength of  $4.5 \times 10^{-14}$  cm, a mean free path in nuclear matter<sup>2</sup> of about  $6 \times 10^{-13}$  cm and a velocity larger than that of nucleon bound in a nucleus. It is thus possible to localize an incoming proton within the target nucleus, and to describe the interaction as one or more successive nucleon-nucleon collisions inside the nucleus. This description predicts<sup>3</sup> the general nature of the scattered proton energy spectrum when a target is bombarded with high-energy protons of a well defined energy. The spectrum at a given angle is expected to contain an elastic peak, an inelastic continuum, and in certain cases a "quasi-elastic" peak.<sup>4</sup> This last type of peak is elastic in the sense that its energy is closely related to that of a proton scattered at the same angle in a free nucleon-nucleon collision, but the peak is inelastic as far as the target nucleus is concerned and its relatively broad width is determined by the momentum distribution of nucleons inside the target nucleus and by secondary collisions.

We have briefly reported the existence of additional inelastic peaks of a different type.<sup>5</sup> These peaks correspond to the excitation of definite energy levels in the target nucleus. Their energy and width are determined by the detailed properties of the target nucleus. This paper reports a study of these peaks at various scattering angles using 96-Mev protons and a carbon target. The experimental set up is described in some detail since it is similar to that used for studies to be reported later of the scattering from other targets.

### II. APPARATUS AND METHOD

#### (A) Experimental Arrangement

The internal cyclotron beam is extracted by multiple Coulomb scattering from an uranium target into a magnetic channel. This scattered beam is then brought out to the experimental area through an evacuated pipe. A series of 3 slits and a deflecting magnet served to collimate the beam so that it had in general the following characteristics at the target position: width  $\frac{3}{8}$  in.; height 1 in.; intensity  $3 \times 10^6$  protons per sec; energy: 96 Mev with slight day by day variations; energy spread:  $\sim 2$  Mev. Careful tests have failed to show any polarization or the presence of a low-energy tail in this beam.

The experimental arrangement is shown in Fig. 1. The beam passed the defining slit, the antiscattering slit, the ionization chamber monitor, and the target in that order. The telescope detected protons scattered from the target. The angle  $\theta$ , made by the telescope-target axis with the beam direction, could be varied. To obtain optimum energy resolution of the system, the targets were set at angle of  $\theta/2$  with respect to the normal to the beam direction. For the small-angle elastic scattering measurements a scattering chamber was used to reduce background.

The telescope consisted of nine counters labeled *A* through *I* in the direction of proton traversal. Each counter consisted of a stilbene crystal about 0.24 g/cm<sup>2</sup> thick which was mounted against an 1P21 photomultiplier. The detailed telescope geometry, shown in Fig. 2, was chosen so as to minimize the problem of loss of protons due to outscattering without at the same time causing too large an increase in the background or in the individual counting rates. The scattered proton beam was defined by the size of the incident beam at the target and the dimensions of crystal *D*. Absorbers were inserted in the telescope in front of crystal *B*. The distance from the target to the defining counter was 15 in. and 30 in. at scattering angles below and above  $35^\circ$ , respectively.

The pulses from the photomultipliers were fed directly into fast double coincidence circuits of the diode bridge type. Seven such circuits were used to

\* Supported by the joint program of the Office of Naval Research and the U. S. Atomic Energy Commission.

<sup>1</sup> R. Serber, Phys. Rev. **72**, 1114 (1947).

<sup>2</sup> T. B. Taylor, Phys. Rev. **92**, 831 (1953).

<sup>3</sup> M. L. Goldberger, Phys. Rev. **74**, 1269 (1948).

<sup>4</sup> Cladis, Hess, and Moyer, Phys. Rev. **87**, 425 (1952).

<sup>5</sup> K. Strauch and F. Titus, Phys. Rev. **95**, 854 (1954).

make  $AC$ ,  $BD$ ,  $AE$ ,  $BF$ ,  $GC$ ,  $HE$ , and  $ID$  coincidences. These fast coincidence outputs were then amplified and fed into slow coincidence circuits whose output corresponded to  $ABCD$ ,  $ABCDE$ ,  $ABCDEF$ ,  $ABCDEF$ ,  $ABCDEF$ ,  $ABCDEF$ ,  $ABCDEF$ , and  $ABCDEF$  coincidence events. Hereafter the name of these coincidences will be abbreviated: for example  $A-H$  stands for  $ABCDEF$ . A similar coincidence system has been described elsewhere in more detail.<sup>6</sup>

In the electronic arrangement just outlined, single counter pulses were fed directly into a fast coincidence circuit with negligible inherent dead time. Only coincidence pulses traveled through circuits with relatively long recovery times. This feature was important in the success of the experiment as will be discussed later. Accidental coincidence events were at all times completely negligible.

The incident beam was monitored by integrating the current collected in the argon filled ionization chamber. This ionization chamber was calibrated against a Faraday cup constructed by Dr. U. Kruse.

The 0.948-g/cm<sup>2</sup> carbon target was of commercial grade with a purity of 99% as determined by spectroscopic analysis. A complete set of telescope absorbers was constructed so that the whole energy range could be covered in convenient steps. These absorbers were made of polyethylene which has a high ratio of stopping power to rms scattering angle. The stopping power of CH<sub>2</sub> was calculated using the tables of Aaron *et al.*,<sup>7</sup> and the result checked experimentally by comparison with the stopping power of aluminum. The agreement was better than 0.5%.

### (B) Telescope Efficiency

The telescope was used to measure the range spectrum of protons scattered from a given target. This range spectrum was obtained by subtracting the observed  $A-D$ ,  $A-E$ ,  $A-F$ ,  $A-G$ ,  $A-H$ , coincidences from each other to get the number of protons stopping

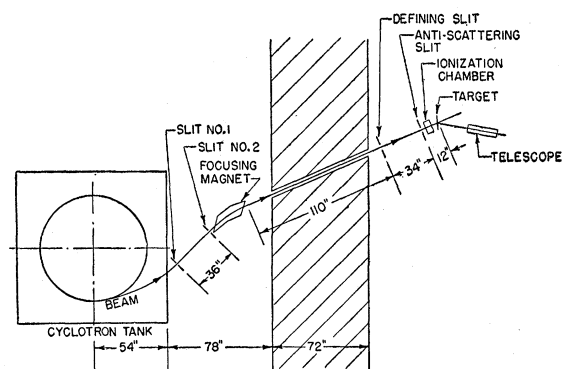


FIG. 1. Experimental arrangement.

<sup>6</sup> K. Strauch, *Rev. Sci. Instr.* **24**, 283 (1953).

<sup>7</sup> Aaron, Hoffman, and Williams, Atomic Energy Commission Report AECU-663 (unpublished).

in counters  $D$ ,  $E$ ,  $F$ , and  $G$ , respectively. Since the amount of material in front of these counters was known it was possible to calculate the range of those particles that stopped in a given counter. The procedure is valid as long as the difference in integral counting rates such as  $A-E$  and  $A-F$  is due to particles stopping in  $E$  and not due to some inefficiency in the  $BF$  channel. It is only because it is possible to set very accurately upper limits to such inefficiency effects in relatively short time intervals by a "difference method" that telescopes are such useful devices to measure energy distributions. The thicknesses of counters  $A$ ,  $B$ , and  $C$  and of the target determined the lowest energy proton that could be detected.

The number of particles that stop in a given counter is often small compared to the total number of particles going through the counter. In a typical case, one proton out of twenty entering counter  $E$  actually stopped in this counter. So that this number of protons stopping in  $E$  could be measured to an accuracy of two percent, it was necessary to make sure that the following counter  $F$  had an "efficiency" of at least 99.9 percent. "Counter efficiency" refers to the efficiency of both the counter and the channel electronics including the final scaler. The efficiency of counter  $F$  was measured by comparing  $ABCDEG$  and  $ABCDEF$  coincidences simultaneously. The telescope geometry was such that each proton that originated in the target and passed through counters  $A$ ,  $D$ , and  $G$  also passed through counter  $F$  and thus any difference between the two coincidence rates was due to inefficiency in the  $F$  counter or associated electronics. Since  $ABCDEG$  and  $ABCDEF$  coincidences registered related events, the statistical uncertainty of the difference arises from the value of the difference, *not* from the value of the integral counts. This fact allows the rapid measurement of efficiencies to the high degree of accuracy required.

The main cause of inefficiency was due to dead time losses in the amplifiers and scalars. For the example just discussed, the beam intensity would have been reduced if necessary until the difference in counting rates between  $ABCDEG$  and  $ABCDEF$  rates amounted to less than 0.1 percent of the integral rates.

The efficiency of all counters but  $D$  and  $I$  could be rapidly measured by this difference method. The efficiency of the defining crystal  $D$  did not seriously

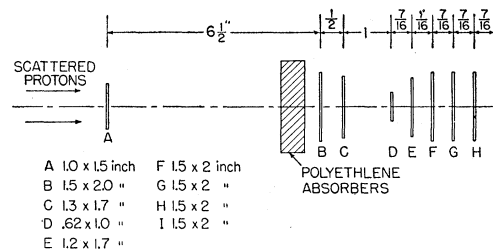


FIG. 2. Telescope geometry.

affect any difference rate, but only the integral rate of protons scattered from the target. It was therefore considered sufficient to assure a better than 98 percent efficiency by taking plateaus of all critical electronic settings. Counter *I* was only used to measure the efficiency of counter *H*.

### (C) Experimental Procedure

In each run the following steps were taken:

(1) The external beam was photographically aligned on the center of the targets and along the  $0^\circ$  axis. The accuracy of this alignment is estimated to be  $\pm 1^\circ$ .

(2) The target and telescope were put at the desired position. The efficiency of the counters was then measured by the "difference method" using the highest counting rates to be encountered. A 99.9% efficiency was required and if necessary the beam intensity was reduced to obtain this efficiency.

(3) With no absorber in the telescope and the target in place, data was taken for a specific charge collected by the ionization chamber. The target was then removed and a background reading taken.<sup>8</sup> An absorber whose stopping power was equivalent to that of scintillators *D*, *E*, *F*, and *G* was then inserted into the telescope and target and background data were taken. Further absorbers of the same thickness were added in turn and similar data collected until all protons stopped in the telescope. A complete range spectrum was obtained in this manner.

(4) Counter efficiencies were checked by the difference method.

(5) An absorber equivalent in stopping power to 1.5 times the average crystal thickness was then inserted into the telescope, and another complete range spectrum taken with the absorbers described in step (3). This second "shifted" spectrum corresponds to ranges midway between those observed in step (3). A point obtained by subtracting the integral rates of two adjacent channels was flanked by points obtained by subtraction of integral rates of different channels. This facilitated the early detection of inefficient counter operation and checked the stability of the equipment.

(6) Counter efficiencies were again checked by the difference method.

The telescope was then shifted to a new angle and steps (3)–(6) were repeated.

### (D) Calculation of Proton Energy Spectra

The observed range spectra were converted into energy spectra by multiplying each point by the inverse stopping power of the corresponding crystal at the energy corresponding to the range. The absolute cross sections were obtained by calibrating the ionization

chamber monitor with a Faraday cup constructed by U. Kruse. The calibration was checked by measuring the *p-p* cross section. Satisfactory agreement with the results of Kruse *et al.*<sup>9</sup> was obtained.

The resulting energy spectra must be corrected for the effect of nuclear absorption of the scattered protons in the telescope. Two types of correction have to be applied. Correction 1 is for the loss of protons which should have stopped in a counter but were absorbed in material in front of this counter: this correction increases the observed cross sections. Correction 2 is for protons which should have passed through a counter but were absorbed in it: this correction decreases the observed cross sections.

Correction 1 has been estimated from the known energy dependence of *p-p* and *p-C* scattering cross sections, assuming a constant value of 0.4 for the ratio of inelastic to total scattering cross section. For the elastically scattered protons, this estimate amounts to 13%, and this value has been experimentally verified within  $\pm 2\%$  statistical uncertainty by measuring the ratio of "with absorber" to "no absorber" telescope counting rates when the telescope was placed directly into a very low intensity external beam. As a result, the theoretical estimate is used to make correction 1.

Correction 2 has been estimated similarly: it is a function of the energy distribution of the scattered protons since the number of protons absorbed in a counter depends on the number and energy of the particles that traverse it. Owing to the presence of high-energy peaks in the observed spectra, corrections 1 and 2 cancel within an accuracy of 2% in the lower energy continuum regions. The angular distributions shown in Fig. 6 have been corrected for telescope absorption.

### (E) Resolution and Errors

The energy resolution of the apparatus for elastic or nearly elastic scattered protons depends primarily on the energy width of the counter scintillators: these averaged 2.2 Mev, a value chosen to be equal to the energy width of the incident beam. Thus a combined resolution width of 3.0 Mev is obtained. For low-energy inelastic protons the energy resolution is determined almost entirely by the difference in energy lost in the target depending on whether the interaction took place in the front or rear section of the target. For 45-Mev protons the energy resolution was only 9 Mev in the laboratory system.

The angular resolution is determined by the geometry of the beam and the defining counter and by multiple scattering in the target. Geometry and target thickness were both varied to obtain reasonable counting rates. As a result, the full width at half-maximum of the resolution function varied from  $0.7^\circ$  for angles smaller than  $15^\circ$  to  $2.7^\circ$  for angles larger than  $30^\circ$ . The full widths are indicated on Figs. 4 and 6.

<sup>8</sup> The background was small enough so that possible differences between target-in and target-out conditions were negligible.

<sup>9</sup> Kruse, Ramsey, and Teem, *Phys. Rev.* **101**, 1079 (1956).

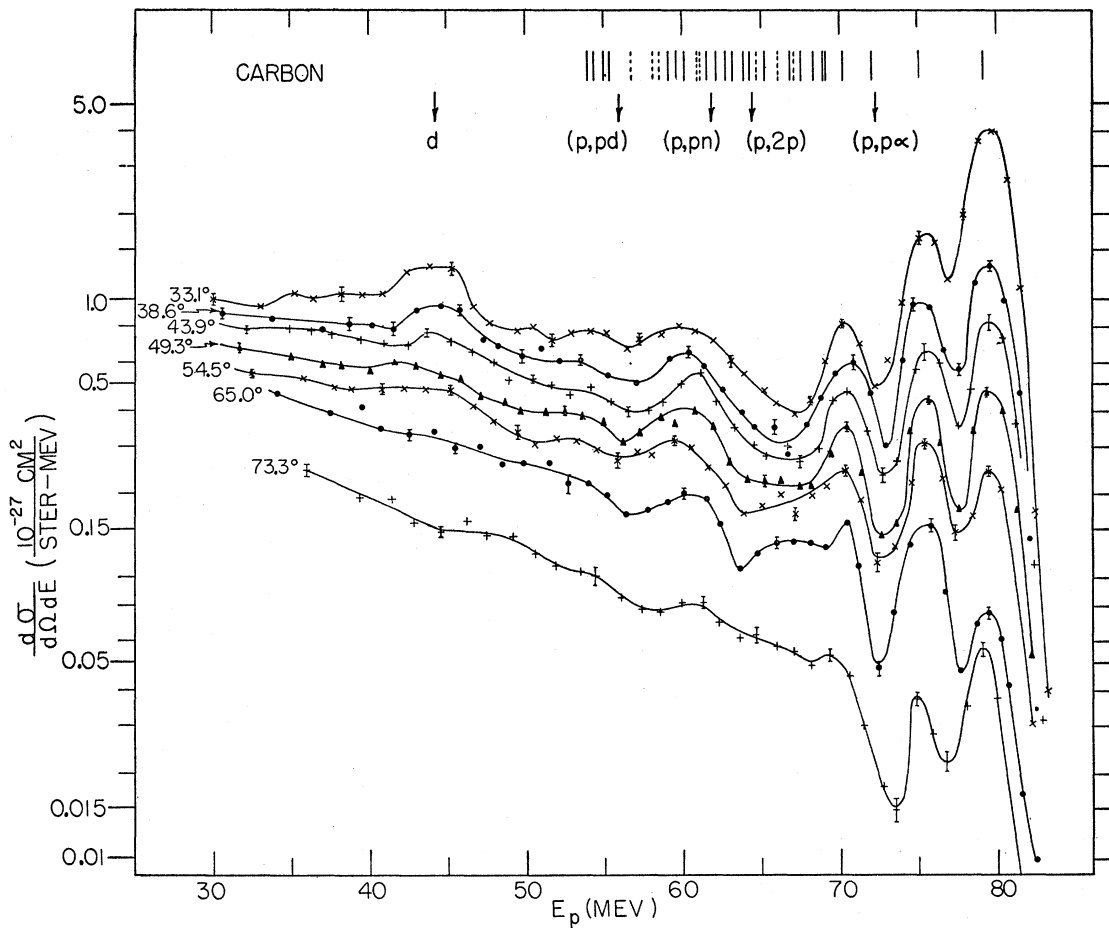


FIG. 3. Energy spectra of scattered protons in the center-of-mass system.

The absolute values of the cross sections are believed to be good to  $\pm 4\%$ . The absolute values of the proton energies are accurate to  $\pm 1.8\%$ .

### III. EXPERIMENTAL RESULTS

Our study consists of two parts. In the first part, complete spectra were taken at seven angles, while the second concentrated on the elastic and first inelastic peak with measurements taken at a much larger number of angles.

Figure 3 shows complete spectra observed at laboratory angles of  $30^\circ$ ,  $35^\circ$ ,  $40^\circ$ ,  $45^\circ$ ,  $50^\circ$ ,  $60^\circ$ , and  $70^\circ$ . These correspond to center-of-mass scattering angles (averaged over the energy region observed) of  $33.1^\circ$ ,  $38.6^\circ$ ,  $43.9^\circ$ ,  $49.3^\circ$ ,  $54.5^\circ$ ,  $65.0^\circ$ , and  $75.3^\circ$ . The incident proton energy averaged 93.0 Mev at the center of the carbon target in the laboratory. All plots are drawn, and unless otherwise stated, all further discussion will be in terms of the proton-carbon center-of-mass system. No corrections for telescope absorption are shown in Fig. 3 to increase readability. Each point represents the average of at least two measurements,

and alternate points were taken at different times using "normal" and "shifted" absorbers (Sec. II). Errors shown are of statistical origin only. Arrows indicate the highest energy a proton could have if it originated in the indicated nuclear reactions. The arrow labeled *d* indicates the energy of protons which have the same range as pickup deuterons that leave the residual nucleus in its ground state. (The telescope measures the range, not the nature, of scattered particles.) Lines indicate the energy of possible inelastically scattered protons that leave the target nucleus  $C^{12}$  in known energy states listed by Ajzenberg and Lauritsen.<sup>10</sup>

Figure 3 shows the existence of peaks at  $79.5 \pm 0.2$  Mev,  $75.4 \pm 0.3$  Mev,  $70.5 \pm 0.3$  Mev,  $60.3 \pm 0.7$  Mev, and  $44 \pm 1$  Mev. In the carbon-proton center-of-mass system, the position of these peaks is independent of the angle of observation. The highest energy peak at  $79.5 \pm 0.2$  Mev in Fig. 3 consists of elastically scattered protons. The peak width is determined by the experimental energy resolution, and the observed widths agree well with the estimates of Sec. II.

<sup>10</sup> F. Ajzenberg and T. Lauritsen, *Revs. Modern Phys.* **27**, 77 (1955).

The  $75.4 \pm 0.3$  Mev peak is formed by inelastically scattered protons, and its position strongly suggests that it corresponds to protons that have excited the target nucleus to its well known 4.43-Mev level. At all angles the width of this peak is similar to that of the elastic peak. This is to be expected since it corresponds to the excitation defined energy level<sup>10</sup> and since its position is above the highest energy proton which could have originated in a three-body disintegration.

The position of the  $70.5 \pm 0.3$  Mev peak suggests that it corresponds to the excitation of the 9.61-Mev level of  $C^{12}$ . At larger angles, the apparent width of this peak is larger than that of the elastic peak: this fact is probably caused by the increasing importance of the inelastic continuum produced in the  $(p, \alpha p)$  reaction, which lies under the inelastic peak. At  $75.3^\circ$  this peak has just about disappeared in the continuum.

A third inelastic peak is seen at  $60.3 \pm 0.7$  Mev. It corresponds to a nuclear excitation of  $20.8 \pm 0.7$  Mev. This peak rides on top of a continuum, and as a result its width is not well determined. The width at  $43.9^\circ$  is consistent with the excitation of one level only, while at some of the other angles it appears rather too broad. At any rate, a preferential excitation of one or more levels in this energy region certainly takes place.

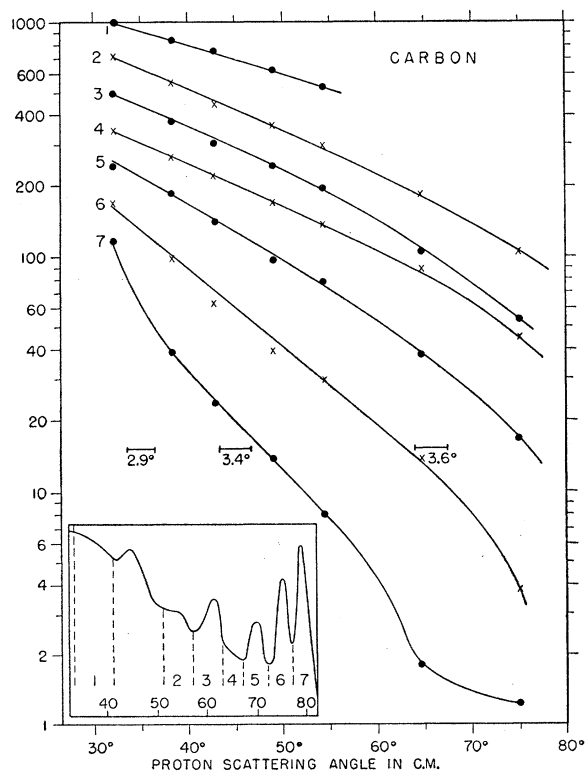


FIG. 4. Angular distribution of proton groups of different energies. The insert shows the energy position and width of these groups. The ordinate scale is different for each curve and was chosen to separate the curves for the sake of clarity. The angular resolution (full width at half-maximum) is indicated.

The low-energy peak at 44-Mev occurs at the energy where pickup deuterons are expected to appear. At  $33.1^\circ$ , we estimate a cross section of not less than 1.8 mb/sterad for the area under the peak. Selove<sup>11</sup> has measured the pickup deuteron cross section accurately and finds  $2.89 \pm 0.30$  mb/sterad at  $33^\circ$ . The width of the 44-Mev peaks is narrower than possible for protons of this energy. It is felt that the position, width, and magnitude of these low-energy peaks support their interpretation as consisting of pickup deuterons.

Below 72.6 Mev, protons that result from the breakup of the target nucleus can appear, and these are expected to have a continuous energy distribution. At the same time, the known distance between levels lying more than 10 Mev above the ground state becomes much smaller than the experimental energy resolution. It is thus impossible to say what fraction of the observed continuum is due to unresolved peaks. The relative importance of the continuum increases as the scattering angle is increased. There is no sharp rise at the  $(p, pn)$  or  $(p, 2p)$  thresholds: rather such a rise occurs at the  $(p, \alpha p)$  threshold.

The angular dependence of the energy distributions is brought out in Fig. 4. A plot is made for each of seven energy sections divided as shown, and the various curves are arbitrarily separated for the sake of clarity. Each curve has thus a different absolute ordinate scale. The cross sections for all proton energy sections decrease rapidly with increasing scattering angle, and only the elastic protons results give an indication of some structure. In general, the higher the energy of the inelastic protons, the steeper the angular decrease. Only group 3 is an exception and this group contains the 60.3-Mev peak: it decreases more rapidly with increasing angle than the continuum on either side. Since only a fraction of the group 3 protons belong to this peak, this result suggests a relatively steep decrease of the number of protons belonging to the 60.3-Mev peak.

With the energy resolution available, the elastic and 75.4-Mev peaks could be separated fairly cleanly from the continuum and from each other. Spectra covering the 70 to 80 Mev region have therefore been obtained in  $2.5^\circ$  steps between  $20^\circ$  and  $40^\circ$ , in  $5^\circ$  steps between  $40^\circ$  and  $80^\circ$ , and one spectrum at  $90^\circ$  (all angles in the laboratory system). This series of measurements was carried out with a 99.5-Mev beam incident on a  $1.37$  g/cm<sup>2</sup> carbon target. The incident energy averaged 94.3 Mev (laboratory system) at the center of the target. Each spectrum has been analyzed in terms of the area lying under each of the two peaks. Three typical examples are shown in Fig. 5. The areas determine the cross sections, after the corrections for telescope absorption have been applied (Sec. II).

Below laboratory angles of  $20^\circ$ , the elastic peak becomes so overwhelmingly large that it becomes

<sup>11</sup> W. Selove, Phys. Rev. **101**, 231 (1956).

difficult to distinguish between inelastically scattered protons, and elastic protons that have been absorbed in the telescope. Therefore only elastic protons have been counted at small angles.  $0.5^\circ$  and  $1^\circ$  steps were used in this region, since the angular resolution could be increased.<sup>12</sup>

The results are shown in Fig. 6. The angular distribution of elastically scattered protons shows the following characteristic features:

- (1) A steep Coulomb scattering region at angles below  $4^\circ$ .
- (2) A small minimum at  $6.5^\circ$  followed by a nearly flat region due to Coulomb-nuclear scattering interference.
- (3) A steadily decreasing cross section with indications of a first diffraction "minimum" at  $40^\circ$  and of a second at  $64^\circ$ .

It should be emphasized that these minima appear only because the inelastic 75.4-Mev peak was separated from the elastic peak. This fact explains the failure to observe diffraction features with C in some previous high-energy experiments.

The angular distribution of inelastic protons leaving the target nucleus in its first excited state shows a smooth behavior. The indication of some structure at  $70^\circ$  is probably not outside the experimental error. At small angles the cross section is much smaller than for elastic protons, while at angles above  $35^\circ$  the elastic and inelastic protons have cross sections of comparable size. The inelastic protons show no structure effects of a magnitude comparable to that of elastic protons. The results shown in Fig. 4 indicate that the angular distribution of protons lying under the 70.5- and 60.5-Mev peaks is similar to that of the protons corresponding to the 75.5-Mev peak shown in Fig. 5. This statement refers of course only to the angular region covered and describes only the general trend since the angular increments of the data presented in Fig. 4 are quite broad. Better energy resolution is required before it is possible to obtain more precise angular distributions for the lower energy inelastic peaks.

#### IV. DISCUSSION

The elastic scattering results reported in the previous section will be considered in detail in a later report covering the elastic scattering from a variety of elements. They are presented here for comparison with the elastic results which will be discussed in some detail.

Studies similar to the one reported here have been carried out by Hecht<sup>13</sup> with 31-Mev protons and by Fregeau and Hofstadter<sup>14</sup> with electrons between 80

to 187 Mev. Hecht finds inelastic peaks corresponding to the excitation of nuclear energy levels at 4.43 Mev, 9.60 Mev, and to weaker extent at 14.98 Mev. Evidence for a level at 21.9 Mev, and of several broad levels between 11 and 20 Mev is also reported. The angular distribution of elastically scattered 31-Mev protons shows more pronounced diffraction minima than the 96 Mev results of Fig. 6. This is not surprising considering the larger nuclear transparency at the higher energy. Hecht finds that the angular distribution of inelastic protons that have excited the carbon nucleus to the 4.43-Mev state shows diffraction features of magnitude similar to his elastic results. This is in contrast to the nearly smooth behavior of the corresponding 96-Mev results of Fig. 6.

Fregeau and Hofstadter report the observation of inelastic peaks corresponding to the excitation of energy levels at 4.43 Mev, 7.68 Mev, and 9.61 Mev. In the forward direction, the relative scattering cross

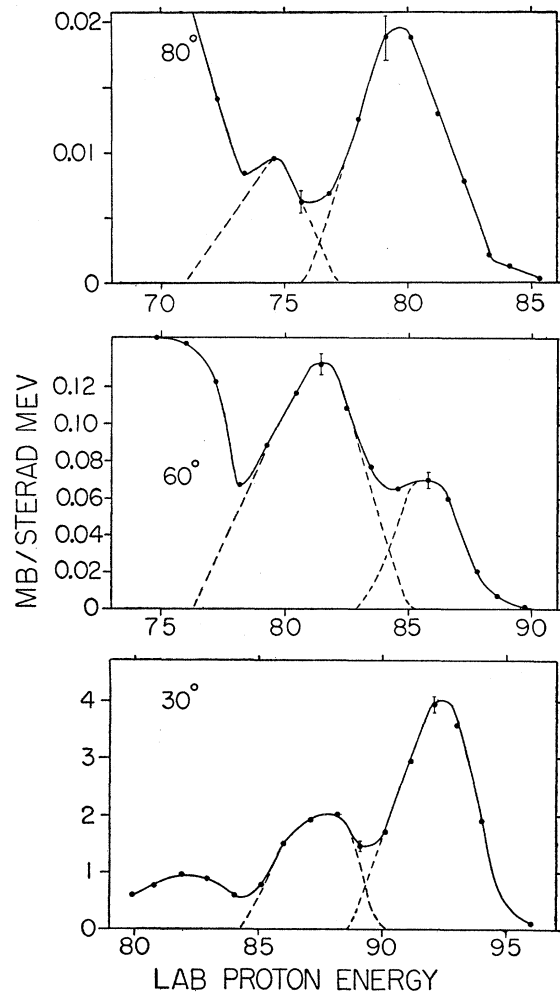


Fig. 5. The high-energy region of the proton spectra at three representative angles. Dashed lines indicate the peak shape used to obtain cross sections.

<sup>12</sup> The small-angle measurements were carried with a slightly modified experimental set up designed specifically for elastic scattering. They are included here for the sake of completeness.

<sup>13</sup> G. J. Hecht, University of California Radiation Laboratory Report UCRL 2969 (unpublished).

<sup>14</sup> J. H. Fregeau and R. Hofstadter, Phys. Rev. **99**, 1503 (1955).

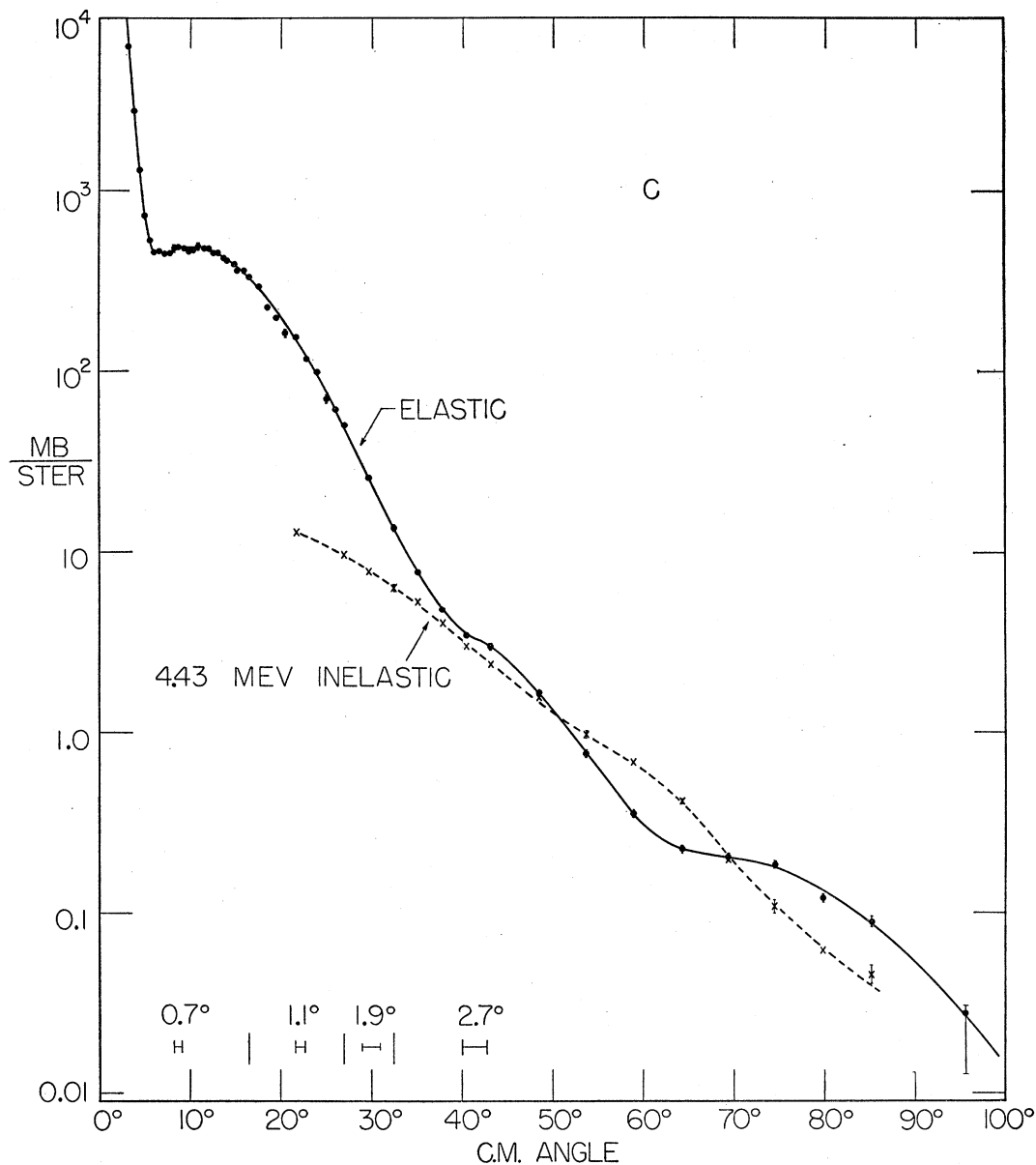


FIG. 6. The angular distribution of elastically scattered protons and inelastically scattered protons that leave the target nucleus in the 4.43-MeV excited state. The plot is in the center-of-mass system. The angular resolution (full width at half-maximum) is indicated.

section decreases with increasing excitation energy of the target nucleus. In the backward direction, the relative order of the cross section for excitation of the 7.68-MeV and 9.61-MeV levels is reversed. In general, the angular distributions of inelastically scattered electrons are less steep than the corresponding data for elastic scattering. The general features of the electron scattering results are quite similar to the proton results reported here, except for the relatively strong excitation of the 7.68-MeV level.

The quoted results and those reported in Sec. III show that for a low- $A$  target such as carbon, inelastic proton scattering that results in the excitation of low-lying energy states is of considerable importance,

at least for energies up to 96 MeV. Using a smooth extrapolation to  $0^\circ$  of the 4.43-MeV inelastic scattering curve of Fig. 6, it is estimated that the cross section for the excitation of the first excited state of  $C^{12}$  represents about 5 percent of the elastic scattering cross section. Such an extrapolation is somewhat uncertain, however it emphasizes the importance of this type of scattering. Any experiment which requires the detection of only elastically scattered protons must therefore have excellent energy discrimination, if angles near and beyond the first diffraction minimum are to be studied.

It is of interest to consider possible methods of excitation of these inelastic peaks. Since their energy position remains constant over a wide angular region

in the proton-carbon center-of-mass system, the peaks are *not* the result of the usual "quasi-elastic" collision with some nuclear subunit. In such collisions, the position of the peaks is mainly determined by the proton-subunit kinematics. The constant energy position of the three inelastic peaks means that they are the product of an interaction in which the final state is determined by the detailed properties of the nucleus as a whole. This result does not preclude the possibility that the primary interaction is of a proton-nucleon or proton-nuclear subunit type, it only means that both collision partners do not behave like free particles.

The inelastic peaks do not seem to be the result of  $C^{13}$  compound nucleus formation and subsequent proton emission, nor of Coulomb-excitation. The first is made improbable by the high energy and consequent large mean free path of the incident proton, the second by the large momenta transferred to the scattered particle. The inelastic peaks seem to be the result of a "direct" nuclear excitation in which the incident particle interacts with the nucleus for a time of the order of  $R/v$ , where  $R$  is the nuclear radius and  $v$  the velocity of the incident proton. The term "direct" excitation is used to emphasize the fact that the excited level is not reached through particle and gamma-ray cascade emission. Several possible methods of excitation suggest themselves from nuclear models that have been found useful in interpreting the properties of light nuclei.<sup>15</sup> Just as certain properties of each of these models probably belong in a complete description of light nuclei, so the inelastic scattering probably results from a combination of the models that will be discussed.

The independent-particle model leads naturally to an interaction model similar to the excitation of atomic states by electron bombardment. The incident proton interacts with one nucleon inside the target nucleus, excites the nucleon into a higher energy state, and then leaves the nucleus without further interaction. The last condition is quite probable, since the mean free path in nuclear matter of 96-Mev protons is about twice as large as the radius of the carbon nucleus. This suggests that there is no need to restrict such collisions to the nuclear surface as was done for lower energy particles by Austern *et al.*<sup>16</sup> The model requires the presence of nucleons inside the target nucleus that have relatively large momenta to make possible the observed large-angle scattering with small energy loss. For instance, a nucleon with an internal kinetic energy of 45 Mev can collide with the incident proton in such a manner that a deflection of  $80^\circ$  is produced and the incident particle emerges with its initial energy reduced by only 4.4 Mev. Such an internal energy is well below the largest values derived by Selove.<sup>11</sup>

This interaction model predicts the strong excitation of those states that can be reached by a single-particle

transition. Examples are single particle states, and all states to which these are strongly coupled. Parentage arguments<sup>17</sup> are then useful in predicting the nature and strength of the probable transitions.

In order to illustrate the type of information that one might hopefully expect to obtain from more accurate and comprehensive data and detailed calculations based on this interaction model, we will consider the information available on the nature of the strongly excited levels according to the individual particle model. If one uses the  $j$ - $j$  coupling description of the shell model, the carbon ground state has an  $s_{\frac{1}{2}}^4 p_{\frac{3}{2}}^8$  configuration. The 4.43-Mev level is known to be  $2^+$  and presumably belongs to the  $s_{\frac{1}{2}}^4 p_{\frac{3}{2}}^7 p_{\frac{1}{2}}^1$  configuration.<sup>15</sup> It can thus be excited by a single-particle transition, and it is found to be strongly excited. The identification of the  $1^+$  state of the same excited configuration with a known level has not been made; taking the interaction model more seriously than is warranted, the 9.61-Mev level suggests itself since it is found to be strongly excited. A  $0^+$  state exists in carbon at 7.68 Mev: it can be produced by a two particle transition to a configuration such as  $s_{\frac{1}{2}}^4 p_{\frac{3}{2}}^6 p_{\frac{1}{2}}^2$  or by a single particle transition to the  $s_{\frac{1}{2}}^3 2s_{\frac{1}{2}}^1 p_{\frac{3}{2}}^8$  configuration.<sup>18</sup> The results shown in the previous section indicate at most a weak excitation of this configuration with 31- and 96-Mev protons as expected if a two-particle transition is involved. None of the  $T=1$  states known above 15 Mev seem to be excited especially strongly, although some at least can be reached by a single particle transition from the ground state.

The next peak corresponds to the excitation of one or more levels grouped around  $20.8 \pm 0.7$  Mev. The reaction model suggests that they are mainly individual particle states, and they might thus belong to the next excited configuration which is  $s_{\frac{1}{2}}^4 p_{\frac{3}{2}}^7 d_{\frac{5}{2}}$ . It is of interest to note that Halpern and Mann<sup>19</sup> have found a strong 1.7-Mev wide resonance at  $21.5 \pm 0.5$  Mev in the  $(\gamma, p)$  cross section, and Mann *et al.*<sup>20</sup> have interpreted angular distribution measurements in terms of the excitation of a single particle level of just this configuration. It seems reasonable to suppose that at least some of the same levels are preferentially excited by  $\gamma$  rays and by high-energy protons.

No detailed calculations based on the individual-particle excitation model have as yet been made for the angular distribution of inelastically scattered 100-Mev protons. Born approximation considerations indicate that the observed distributions are in general agreement with this reaction model, and that dips are possible in the forward direction where no datum is as yet available, and where it is difficult to obtain.

While the preceding discussion has been limited to an initial proton-nucleon interaction, the model should

<sup>17</sup> A. M. Lane and D. H. Wilkinson, *Phys. Rev.* **97**, 1192 (1955).

<sup>18</sup> P. J. Redmond, *Phys. Rev.* **101**, 751 (1956).

<sup>19</sup> J. Halpern and A. K. Mann, *Phys. Rev.* **83**, 370 (1951).

<sup>20</sup> Mann, Stephens, and Wilkinson, *Phys. Rev.* **97**, 1184 (1955).

<sup>15</sup> D. R. Inglis, *Revs. Modern Phys.* **25**, 390 (1953).

<sup>16</sup> Austern, Butler, and McManus, *Phys. Rev.* **92**, 350 (1953).



be enlarged by including other nuclear subunits as possible targets. Thus the alpha-particle model<sup>15</sup> of  $C^{12}$  suggests alpha-particle targets: the rapid increase at large angles (Fig. 3) of the apparent continuum above the  $(p, \alpha p)$  threshold supports the existence of such collisions. Nor can excitation modes of the nucleus as a whole be excluded.

The shape, cross section, and angular variation of the inelastic continuum are in general agreement with the corresponding neutron spectra.<sup>21</sup>

### V. CONCLUSION

It has been found that important contributions to inelastic scattering of 96-Mev protons arise from the excitation of nuclear energy states in the target nucleus. The results presented show the excitation of levels at 4.43, 9.61, and 20.8 Mev and indicate that the corresponding excitation cross sections decrease smoothly with increasing scattering angle. Further work with better energy resolution is clearly indicated. Besides the intrinsic interest of this type of investigation for a more complete understanding of the mechanism of

<sup>21</sup> J. A. Hofmann and K. Strauch, Phys. Rev. **90**, 449 (1953).

high-energy nuclear reactions, the high energy and consequent short interaction time and large mean free path in nuclear matter of the scattered proton would seem to favor simple rearrangements of the ground state structure. This might make it possible to obtain information on the nature of excited states which cannot as easily be obtained from lower energy results. Since it has been found possible to obtain polarized proton beams at 140 Mev and higher energies, inelastic proton scattering leading to the excitation of nuclear levels should become possible with polarized protons. These results also emphasize the fact that any experiment in which only elastically scattered particles are to be detected requires good energy resolution.

### ACKNOWLEDGMENTS

We wish to thank G. P. Calame, F. Federighi, and J. Niederer for help in taking data and calculating the spectra. G. Gerstein is responsible for the small angle elastic scattering data and we appreciate his permission to include them in this report. This work would not have been possible without the fine cooperation of the entire staff of the cyclotron laboratory.

## Production of a $\theta^0$ Particle without an Associated Hyperon in a $\pi^- - p$ Collision\*

WILLIAM B. FOWLER, GEORGE MAENCHEN, WILSON M. POWELL, GEORGE SAPHIR,† AND ROBERT W. WRIGHT  
Radiation Laboratory and Department of Physics, University of California, Berkeley, California  
(Received March 27, 1956)

An event is described that is interpreted as evidence for the simultaneous production of a  $\theta^0$  and a  $\bar{\theta}^0$  according to the scheme of Gell-Mann and Pais. This interpretation assumes the production of a normal  $\theta^0$  and a  $K^0$  with no associated hyperon, where the  $\theta^0$  is observed and the  $K^0$  is inferred from the rule of associated production of heavy unstable particles. The event was obtained by exposing a high-pressure diffusion cloud chamber to a 4.5-Bev/c  $\pi^-$  meson beam from the Bevatron. The event is most reasonably interpreted as  $\pi^- + p \rightarrow \pi^- + p + \theta^0 +$  (neutral). Energy and momentum conservation are satisfied by an undetected neutral particle having a mass of  $502_{-124}^{+91}$  Mev. This is consistent with the associated production of a  $\theta^0$  and a  $\bar{\theta}^0$  according to the scheme of Gell-Mann and Pais. Details are given and alternative interpretations are discussed.

**D**URING an investigation of the interactions of 4.5-Bev/c  $\pi^-$  mesons with protons,<sup>1</sup> an interesting event involving the production and decay of a  $\theta^0$  was observed. Most of the previously reported<sup>2</sup> examples of production of heavy unstable particles in  $\pi^- - p$  collisions were interpreted as due to the associated production of a  $K$  meson and a hyperon. An exception is the

event obtained by Ceccarelli, Grilli, Merlin, Salandin, and Sechi<sup>3</sup> in the  $G$ -stack which is interpreted as  $\pi^- + p \rightarrow K^+ + K^- + n$ . The event to be described also is not consistent with the associated production of a  $K$  meson and a hyperon and is most readily explained as the production of two neutral  $K$  particles.

The general experimental arrangement is shown in Fig. 1. The  $\pi^-$  mesons were produced by circulating protons of 5.7 Bev striking a carbon target inside the Bevatron. Mesons emitted in the forward direction underwent momentum analysis by deflections of  $17.6^\circ$  in the magnetic field of the Bevatron and  $10.8^\circ$  in an

\* This work was performed under the auspices of the U. S. Atomic Energy Commission.

† Also at the University of San Francisco.

<sup>1</sup> Maenchen, Powell, Saphir, and Wright, Phys. Rev. **99**, 1619 (1955).

<sup>2</sup> Fowler, Shutt, Thorndike, and Whittemore, Phys. Rev. **91**, 1287 (1953); **93**, 861 (1954); and **98**, 121 (1955). W. D. Walker, Phys. Rev. **98**, 1407 (1955); W. D. Shephard and W. D. Walker, Phys. Rev. **100**, 1264 (1955).

<sup>3</sup> Ceccarelli, Grilli, Merlin, Salandin, and Sechi, Nuovo cimento **2**, 828 (1955).